DRAFT VERSION JULY 28, 1999
Preprint typeset using LaTeX style emulateapj v. 04/03/99

MOLECULAR GAS IN THE POWERFUL RADIO NUCLEUS OF THE ULTRALUMINOUS INFRARED GALAXY PKS 1345+12

A. S. EVANS[1,2], D. C. KIM[3,4], J. M. MAZZARELLA[3], N. Z. SCOVILLE[1],
AND
D. B. SANDERS[6]

Draft version July 28, 1999

ABSTRACT

Millimeter CO($1 \rightarrow 0$) interferometry and high resolution, *Hubble Space Telescope* (HST) 1.1, 1.6, and 2.2 μm imaging of the radio compact galaxy PKS 1345+12 are presented. With an infrared luminosity of $\sim 2\times10^{12}$ $L_\odot$, PKS 1345+12 is a prime candidate for studying the link between the ultraluminous infrared galaxy phenomenon and radio galaxies. These new observations probe the molecular gas distribution and obscured nuclear regions of PKS 1345+12 and provide morphological support for the idea that the radio activity in powerful radio galaxies is triggered by the merger of gas rich galaxies. Two nuclei separated by 2″ (4.0 kpc) are observed in the near-infrared; the extended southeastern nucleus has colors consistent with reddened starlight, and the compact northwestern nucleus has extremely red colors indicative of an optical quasar with a warm dust component. Further, the molecular gas, 3mm continuum, and radio emission are coincident with the redder nucleus, confirming that the northwestern nucleus is the site of the AGN and that the molecular gas is the likely fuel source.

Subject headings: galaxies: ISM—infrared: galaxies—ISM: molecules—radio lines: galaxies—galaxies: active—individual: PKS 1345+12

1. INTRODUCTION

Almost all ultraluminous infrared galaxies [ULIGs: $L_{IR}(8-1000\mu m) \geq 1\times10^{12}$ $L_\odot$] have optical/near-infrared morphologies indicative of galaxy-galaxy mergers (e.g. Joseph & Wright 1985; Armus, Heckman, & Miley 1987; Sanders et al. 1988a; Murphy et al. 1996; Kim 1995). Their large quantities of dust and molecular gas (e.g., Sanders, Scoville, & Soifer 1991; Solomon et al. 1997), as well as evidence of abundant young star clusters in many ULIGs (e.g. Surace et al. 1998), are strong evidence of recent/ongoing star formation. Molecular gas is also a likely source of fuel for active galactic nuclei (AGN) such as quasars and radio galaxies, many of which have high L_{IR} and disturbed optical morphologies (e.g., Stockton & MacKenty 1983; MacKenty & Stockton 1984; Heckman et al. 1986; Smith & Heckman 1989a,b), thus providing a possible connection between mergers and the building of supermassive nuclear black holes.

PKS 1345+12 (IRAS 13451+1232: $L_{IR} = 1.7\times10^{12}$ $L_\odot$) is a prime candidate for the link between the ULIG phenomenon and radio galaxies. With a radio luminosity of $P_{408MHz} = 2.4\times10^{26}$ W Hz^{-1}, it is the most powerful radio galaxy detected in CO($1 \rightarrow 0$) to date. It also belongs to a family of "warm" ($f_{25\mu m}/f_{60\mu m} \geq 0.2$, similar to the colors of Seyfert galaxies: de Grijp, Miley, & Lub 1987) infrared galaxies believed to be in a transition state between the "cold" ($f_{25\mu m}/f_{60\mu m} < 0.2$) ULIG phenomenon, when rampant star-formation is occuring and the accretion disk is forming around the nuclear black hole, and the optical quasar phase (Sanders et al 1988a,b). It is observed to have two nuclei with a projected separation of $\sim 2''$ ($\sim$4 kpc: Heckman et al. 1986; Smith & Heckman 1989a,b; Kim 1995), a very compact radio jet ($0.1'' \sim 200$ pc), and an extremely high molecular gas mass (4.4×10^{10} $M_\odot$:[7] Mirabel, Sanders, & Kazes 1989). The ratios of the narrow optical emission lines in PKS 1345+12 indicate that it contains a Seyfert 2 nucleus (Sanders et al. 1988b; Veilleux et al. 1995). Further, recent near-infrared spectroscopic observations have detected broad ($\Delta v_{FWHM} \sim 2600$ km s^{-1}) Paα emission, indicating the presence of a quasar nucleus which is obscured at optical wavelengths (Veilleux, Sanders, & Kim 1997).

The near-infrared spectroscopy of PKS 1345+12 illustrates the importance of probing the nature and distribution of obscured nuclear energy sources in ULIGs at near-infrared wavelengths. Such studies also complement CO interferometry, which provides spatial and kinematic information of the molecular gas reservoirs in these dusty systems. In this *Letter*, the superior resolution of the HST[8] Near-Infrared Camera and Multi-Object Spectrometer (NICMOS: 0.1–0.2″ resolution at 1–2 μm) and the

[1]Division of Physics, Math, & Astronomy, California Institute of Technology, Pasadena, CA 91125
[2]Email Address: ase@astro.caltech.edu
[3]Infrared Processiong & Analysis Center, California Institute of Technology, MS 100-22, Pasadena, CA 91125
[4]Present Address: Academia Sinica Institute of Astronomy & Astrophysics P.O. Box 1-87, NanKang Taipei 115, Taiwan, R. O. C.
[5]UCO/Lick Observatory, University of California, Santa Cruz, CA 95064
[6]Institute for Astronomy, 2680 Woodlawn Drive, Honolulu, HI 96822
[7]Assuming an L'_{CO} to M_{H_2} conversion factor of 4 $M_\odot$ (K km s^{-1} pc^2)$^{-1}$; see §3.
[8]The NASA/ESA Hubble Space Telescope is operated by the Space Telescope Science Institute managed by the Association of Universities for Research in Astronomy Inc. under NASA contract NAS5-26555.

Owens Valley Millimeter Array[9] ($\sim 2''$ resolution at 3 mm) are used to show for the first time the spatial coincidence of the molecular gas and the radio-loud nucleus of PKS 1345+12. These observations provide further support for the relationship between mergers, molecular gas, and AGN activity. An $H_0 = 75$ km s^{-1} Mpc^{-1} and $q_0 = 0.0$ are assumed throughout such that $1''$ subtends ~ 2.0 kpc at the redshift of the galaxy ($z = 0.1224$).

2. OBSERVATIONS AND DATA REDUCTION

2.1. *NICMOS Observations*

HST NICMOS observations of PKS 1345+12 were obtained as part of a larger program to image infrared-luminous galaxies (Scoville et al. 1999; Evans 1999a). Observations were obtained in a single orbit on 1997 December 5 using camera 2, which consists of a 256 × 256 array with pixel scales of $0.0762''$ and $0.0755''$ per pixel in x and y, respectively, providing a $\sim 19.5'' \times 19.3''$ field of view (Thompson et al. 1998). Images were obtained using the wide-band filters F110W (1.10μm, $\Delta\lambda_{\rm FWHM} \sim 0.6\mu$m), F160W (1.60 μm, $\Delta\lambda_{\rm FWHM} \sim 0.4\mu$m), and F222M (2.22 μm, $\Delta\lambda_{\rm FWHM} \sim 0.14\mu$m), which provide a resolution (FWHM) of $0.11''$, $0.16''$, and $0.22''$, respectively. The basic observation and data reduction procedures are the same as those described in Scoville et al. (1999); the total integration times per filter setting for these observations were 480 sec (1.1 and 1.6 μm) and 600 sec (2.2 μm). Flux calibration of the images were done using the scaling factors 2.03×10^{-6}, 2.19×10^{-6}, and 5.49×10^{-6} Jy (ADU/sec)$^{-1}$ at 1.10, 1.60, and 2.22 μm, respectively. The corresponding magnitudes were calculated using the zeropoints 1775, 1083, and 668 Jy (Rieke 1999).

2.2. *Interferometric Observations*

Aperture synthesis maps of CO(1 → 0) and 2.7 mm continuum emission in PKS 1345+12 were made with the Owens Valley Radio Observatory (OVRO) Millimeter Array during five observing periods from 1996 September to 1997 May. The array consists of six 10.4 m telescopes, and the longest observed baseline was 242 m. Each telescope was configured with 120 × 4 MHz digital correlators. During the observations, the nearby quasar HB89 1413+135 (1.5 Jy at 103 GHz; $14^{\rm h}13^{\rm m}33.92^{\rm s}$ $+13°34'17.51''$ [B1950.0]) was observed every 25 minutes to monitor phase and gain variations, and 3C 273 and 3C 454.3 were observed to determine the passband structure. Finally, flux calibration observations of Uranus were obtained.

The OVRO data were reduced and calibrated using the standard Owens Valley data reduction package MMA (Scoville et al. 1992). The data were then exported to the mapping program DIFMAP (Shepherd, Pearson, & Taylor 1995).

3. RESULTS

The reduced 1.1, 1.6, and 2.2 μm images are shown in Figure 1a-c. The galaxy consists of two nuclei with a projected separation of $2.0''$ (4 kpc). Low level surface brightness emission envelops both nuclei, with an east-west extent of $11''$ (22 kpc; full width at 0.5% the maximum flux density at 1.1 and 1.6 μm), and a $5.5''$ (11 kpc) southern extent beyond the southeastern nucleus (hereafter PKS 1345+12SE). The radial surface brightness profile does not constrain the nature of the progenitor galaxies or the type of galaxy they are evolving into; both an $r^{0.25}$ law and an exponential disk give reasonable fits to the profile (see also Scoville et al. 1999).

PKS 1345+12SE is observed to be extended at all three wavelengths with a FWHM of $0.15''$ (300 pc) at 1.1 μm. The measured $1.1''$ aperture magnitudes are 16.86, 15.85, and 15.31 at 1.1, 1.6, and 2.2 μm, respectively, and the derived colors are thus $m_{1.1-1.6}$ =1.01 and $m_{1.6-2.2}$ = 0.54. In contrast, the northwestern nucleus (hereafter PKS 1345+12NW) is unresolved with a FWHM of $0.11''$ (220 pc) at 1.1 μm and magnitudes of 16.66, 15.45, and 13.96 at at 1.1, 1.6, and 2.2 μm, respectively. The near-infrared colors of PKS 1345+12NW are extremely red; $m_{1.1-1.6}$ =1.20 and $m_{1.6-2.2}$ = 1.49. The red nature of PKS 1345+12NW relative to PKS 1345+12SE is also evident in the $1.1''$-aperture flux density ratios of the two nuclei; f(SE)/f(NW) decreases from a value of 0.82 at 1.1 μm to 0.29 at 2.2 μm.

Both the CO(1 → 0) emission and underlying 2.7 mm continuum in PKS 1345+12 are unresolved. The continuum flux density is 0.31 Jy and is consistent with a power-law extrapolation of the radio flux density (e.g. Steppe et al. 1995). The CO emission (Figure 2) has a $\Delta v_{\rm FWHM} \sim 600$ km s^{-1}, a flux density of 14±4 Jy km s^{-1}, and a CO luminosity of $L'_{\rm CO} = 8.2 \times 10^9$ K km s^{-1} pc^2. Thus, the line profile and luminosity are consistent with those derived from NRAO 12m Telescope observations of PKS 1345+12 (i.e., $L'_{\rm CO} = 1.1 \times 10^{10}$ K km s^{-1} pc^2: Mirabel et al. 1989), and confirms that the flux measured in the single-dish observations (i.e., $81''$ FWHM beam) is entirely recovered with OVRO ($\sim 2.2''$ synthesized beam). Assuming a standard ratio (α) of CO luminosity to H_2 mass of 4 $M_\odot$ (K km s^{-1} pc^2)$^{-1}$, which is similar to the value determined for the bulk of the molecular gas in the disk of the Milky Way (Scoville & Sanders 1987; Strong et al. 1988), the molecular gas mass is calculated to be 3.3×10^{10} $M_\odot$, or 14 times the molecular gas mass of the Milky Way.[10] Finally, using the FWHM beam of the CO map ($2.2''$), the molecular gas concentration is calculated to be >2000 $M_\odot$ pc^{-2}, or >15–1500 times that observed in local early-type spiral galaxies (e.g., Young & Scoville 1991) and comparable to the concentrations observed in a sample of luminous infrared galaxies observed by Scoville et al. (1991) and Bryant & Scoville (1999).

4. ASTROMETRY OF THE NEAR-INFRARED IMAGES

The interpretation of the data presented in this *Letter* depends on accurate astrometry of the multiwavelength images. To determine the coordinates of the two nuclei of PKS 1345+12, the positions of stars within 3.5′ of the galaxy were first retrieved from the USNO-A1.0 database. A plate solution (world coordinate system) was then derived for a $7' \times 7'$ R-band image (Kim 1995), which also

[9]The Owens Valley Millimeter Array is a radio telescope facility operated by the California Institute of Technology and is supported by NSF grants AST 93-14079 and AST 96-13717.

[10]Radford, Solomon, & Downes (1991) have used theoretical models to determine that α ranges from 2–5 $M_\odot$ for a reasonable range of temperatures and densities, thus the molecular gas mass of PKS 1345+12 may actually be as low as 1.6×10^{10} $M_\odot$.

shows the two nuclei of PKS 1345+12, using the IRAF task PLTSOL.

The coordinates of the two nuclei, along with the positions of the CO and radio emission from the galaxy, are listed in Table 1. The radio and CO emission appear to be spatially coincident with PKS 1345+12NW - the measured near-infrared peak of PKS 1345+12NW is displaced 0.3″ NE of the radio emission, but is within the uncertainties associated with the positions of the stars used to derive the position of the PKS 1345+12 nuclei. Likewise, the measured near-infrared peak of PKS 1345+12NW is displaced 0.44″ NE of the CO emission and continuum centroids, consistent with the measured OVRO beamsize (see Figure 1d).

5. DISCUSSION

The bulk of the activity in PKS 1345+12 is associated with PKS 1345+12NW. The derived NICMOS colors of the two nuclei provides further support that the AGN resides in PKS 1345+12NW. While the colors of PKS 1345+12SE are consistent with starlight reddened by 1–5 magnitudes of dust, PKS 1345+12NW has colors similar to other warm ULIGs observed with NICMOS - i.e., similar to optically-selected quasars with a 500–1000 K dust component (see also Scoville et al. 1999 and the summary in Evans 1999a). Similar results are derived from near-infrared ground-based observations of PKS 1345+12 (e.g., Surace & Sanders 1999), and recent, high-resolution near-infrared spectroscopy (Veilleux & Sanders 1999) confirm that PKS 1345+12 is the source of the broad-lines detected by Veilleux, Sanders, & Kim (1997).

The presence of a large and concentrated reservoir of molecular gas in PKS 1345+12NW is consistent with the notion that this gas is a source of fuel for the radio phenomenon (e.g., Mirabel et al. 1989). In this scenario, the molecular gas in the western galaxy is driven inward via gravitational instabilities induced by interactions with PKS 1345+12SE.

Of all of the radio galaxies detected in CO($1 \rightarrow 0$) to date (Phillips et al. 1987; Mirabel et al. 1989; Mazzarella et al. 1993; Evans 1999b; Evans et al. 1999), PKS 1345+12 is the most molecular gas-rich, and the only one that clearly has two nuclei. Thus, while PKS 1345+12 is an advanced merger in terms of its relatively small nuclear separation, the fact that the stellar nuclei are 4 kpc apart implies that this system is dynamically younger than the other radio galaxies observed. If the assumption is made that the nuclei of PKS1345+12 are gravitationally bound, the relative velocity of the merging galaxies is $|v| \lesssim (GM_{\rm gal}/R_{\rm sep})^{1/2} \lesssim 300$ km s^{-1}, where $M_{\rm gal} = 10^{11}$ M$_\odot$ and $R_{\rm sep} \sim 4$ kpc, and thus the merger has at least an additional $\sim 10^7$ years before the nuclei coalesce.

From the extent of the radio emission, it is also clear that the jet activity commenced fairly recently. In the 2.3 and 8.5 GHz radio maps shown in Fey, Clegg, & Fomalont (1996), the radio jet has a maximum extent of 0.10″ ($\sim$ 200 pc). Thus, if the jet propagates at a speed of 0.1c, it can be no more than 7000 years old. For comparison, the linear extent of the jets associated with single-nuclei radio galaxies detected in CO are 10–200 kpc, but their estimated jet ages ($\lesssim 10^7$ years) are significantly less than the timescale of the merger process (10^9 years). The creation of the radio jets so late in the life of the merger can be understood in terms of merger dynamics - there will be a natural offset in the time at which the merger begins and the AGN activity occurs because of the time it takes for the molecular gas to agglomerate in the nuclear regions of the galaxy. Further, depending on how typical such a delay is in radio galaxies, the consumption of molecular gas by extended star formation may be well underway prior to the onset of the radio activity, and may continue for another 10^7 years or so. This provides a natural explanation of why radio galaxies with older, extended jets are not observed to have large reservoirs of molecular gas (i.e., $M(\rm H_2) \lesssim 10^9$ M$_\odot$: Mazzarella et al. 1993; Evans 1999b).

We thank the staff of the Owens Valley Millimeter array and the NICMOS GTO team for their support both during and after the observations were obtained, and the referee Sylvain Veilleux for many useful suggestions. ASE also thanks M. Shepherd, D. Frayer, and J. Surace for useful discussion and assistance. ASE was supported by NASA grant NAG 5-3042. J.M.M. and D.-C.K. were supported by the Jet Propulsion Laboratory, California Institute of Technology, under contract with NASA.

REFERENCES

Armus, L., Heckman, T. M. & Miley, G. H. 1987, AJ, 94, 831
Bryant, P. M. & Scoville, N. Z., ApJ, in press
Evans, A. S. 1999a, Ap&SS, in press (astro-ph/9903272)
Evans, A. S. 1999b, in Highly Redshifted Radio Lines, ed. C. Carilli, S. J. E. Radford, K. Menten, & G. Langston (San Francisco: PASP), 156, 74
Evans, A. S., Sanders, D. B., Mazzarella, J. M., & Surace, J. A. 1999, ApJ, 511, 730
Fey, A. L., Clegg, A. W., & Fomalont, E. B. 1996, ApJS, 105, 299
de Grijp, M. H. K., Miley, G. K., & Lub, J. 1987, A&AS, 70, 95
Heckman, T. M. et al. 1986, ApJ, 311, 525
Joseph, R.D. & Wright, G.S. 1985, MNRAS, 214, 87
Kim, D.-C. 1995, PhD Thesis, University of Hawaii at Manoa
Ma, C. 1998, AJ, 116, 516
MacKenty, J. W. & Stockton, A. 1984, ApJ, 283, 64
Mazzarella, J. M., Graham, J. R., Sanders, D. B., & Djorgovski, S. 1993, ApJ, 409, 170
Mirabel, I. F., Sanders, D. B., & Kazès, I. 1989, ApJ, 340, 19
Murphy, T. W., Armus, L., Matthews, K., Soifer, B. T., Mazzarella, J. M. & Neugebauer, G. 1996, AJ, 111, 1025
Phillips, T. G. et al. 1987, ApJ, 322, L33
Radford, S. J. E., Solomon, P. M., & Downes, D. 1991, ApJ, 368, L15
Rieke, M. 1999, in prep.
Sanders, D. B., Scoville, N. Z., & Soifer, B. T. 1991, ApJ, 370, 158
Sanders, D.B., Soifer, B.T., Elias, J.H., Madore, B.F., Matthews, K., Neugebauer, G., & Scoville, N.Z. 1988a, ApJ, 325, 74
Sanders, D.B., Soifer, B.T., Elias, J.H., Neugebauer, G. & Matthews, K. 1988b, ApJ, 328, L35
Scoville, N. Z. et al. 1999, AJ, submitted
Scoville, N. Z., Carlstrom, J. C., Chandler, C. J., Phillips, J. A., Scott, S. L., Tilanus, R. P., & Wang, Z. 1992, PASP, 105, 1482
Scoville, N. Z. & Sanders, D. B. 1987, in Interstellar Processes, ed. D. Hollenbach & H. Thronson (Dordrecht: Reidel), 21
Scoville, N. Z., Sargent, A. I., Sanders, D. B., & Soifer, B. T. 1991, ApJ, 366, L5
Shepherd, M. C., Pearson, T. J., & Taylor, G. B. 1995, BAAS, 27, 903
Smith, E. P. & Heckman, T. M. 1989a, ApJ, 341, 658
Smith, E. P. & Heckman, T. M. 1989b ApJS, 69, 365
Solomon, P. M., Downes, D., Radford, S., & Barrett, J. W. 1997, ApJ, 478, 144

Steppe, H., Jeyakumar, S., Saikia, D. J. & Salter, C. J. 1995, A&AS, 113, 409
Stockton, A. & MacKenty, J. W. 1983, Nature, 305, 678
Strong, A. W. et al. 1988, A&A, 207, 1
Surace, J. A. & Sanders, D. B. 1999, ApJ, 512, 162
Surace, J. A., Sanders, D. B., Vacca, W. D., Veilleux, S., & Mazzarella, J. M. 1998, ApJ, 492, 116
Thompson, R. I, Rieke, M., Schneider, G., Hines, D. C., Corbin, M. R. 1998, ApJ, 492, L95
Veilleux, S., Kim, D.-C., Sanders, D. B., Mazzarella, J. M., & Soifer, B. T. 1995, ApJS, 98, 171
Veilleux, S. & Sanders, D. B. 1999, in preparation
Veilleux, S., Sanders, D. B., & Kim, D.-C. 1997, ApJ, 484, 92
Young, J. S. & Scoville, N. Z. 1991, ARAA, 29, 581

Figure Captions

Figure 1. (a–c) *HST* NICMOS 1.1, 1.6, and 2.2 μm images of PKS 1345+12. The images have peak intensities of 7.5, 11, and 29 μJy for the 1.1, 1.6, and 2.2 μm images, respectively. The speckle pattern surrounding PKS 1345+12NW at 2.2 μm is a PSF artifact. (d) Continuum-subtracted CO($1 \rightarrow 0$) emission superimposed on the false-color NICMOS image. The NICMOS data are displayed with blue as 1.1 μm, green as 1.6 μm, and red as 2.2 μm. The CO data are plotted as 50%, 60%, 70%, 80%, 90%, and 99%, where 50% corresponds to 3.9σ rms and 100% corresponds to a peak flux of 0.0339 Jy/beam. The CO emission is unresolved, with a beam FWHM of 2.46×1.95 at a position angle of -70.5°.

Figure 2. Extracted CO($1 \rightarrow 0$) spectrum of PKS 1345+12. The spectrum is smoothed with a $\sim$ 80 km s^{-1} filter and sampling of 40 km s^{-1} intervals ($S_{\rm rms} \sim 0.005$ Jy).

TABLE 1
PEAKS OF OPTICAL-TO-RADIO EMISSION IN PKS 1345+12

Source	RA (B1950.0)	Dec
13451+1232SE	13:45:06.37	12:32:20.31
13451+1232NW	13:45:06.24	12:32:20.71
2.3/8.4 GHz Radio[1]	13:45:06.22	12:32:20.55
3mm/CO($1 \rightarrow 0$)	13:45:06.21	12:32:20.31

[1]The radio coordinates are taken from Ma (1998).

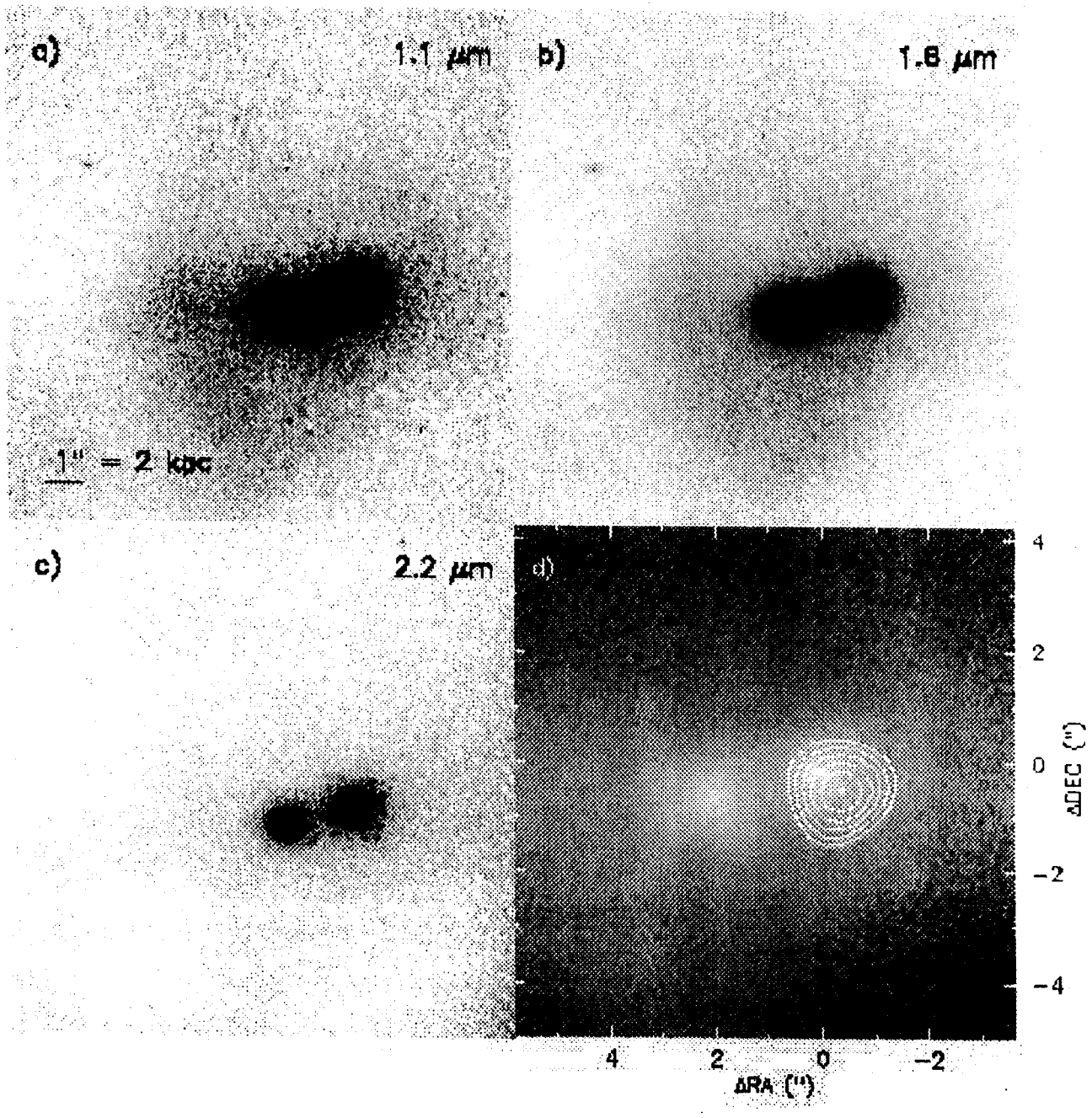

Fig. 1

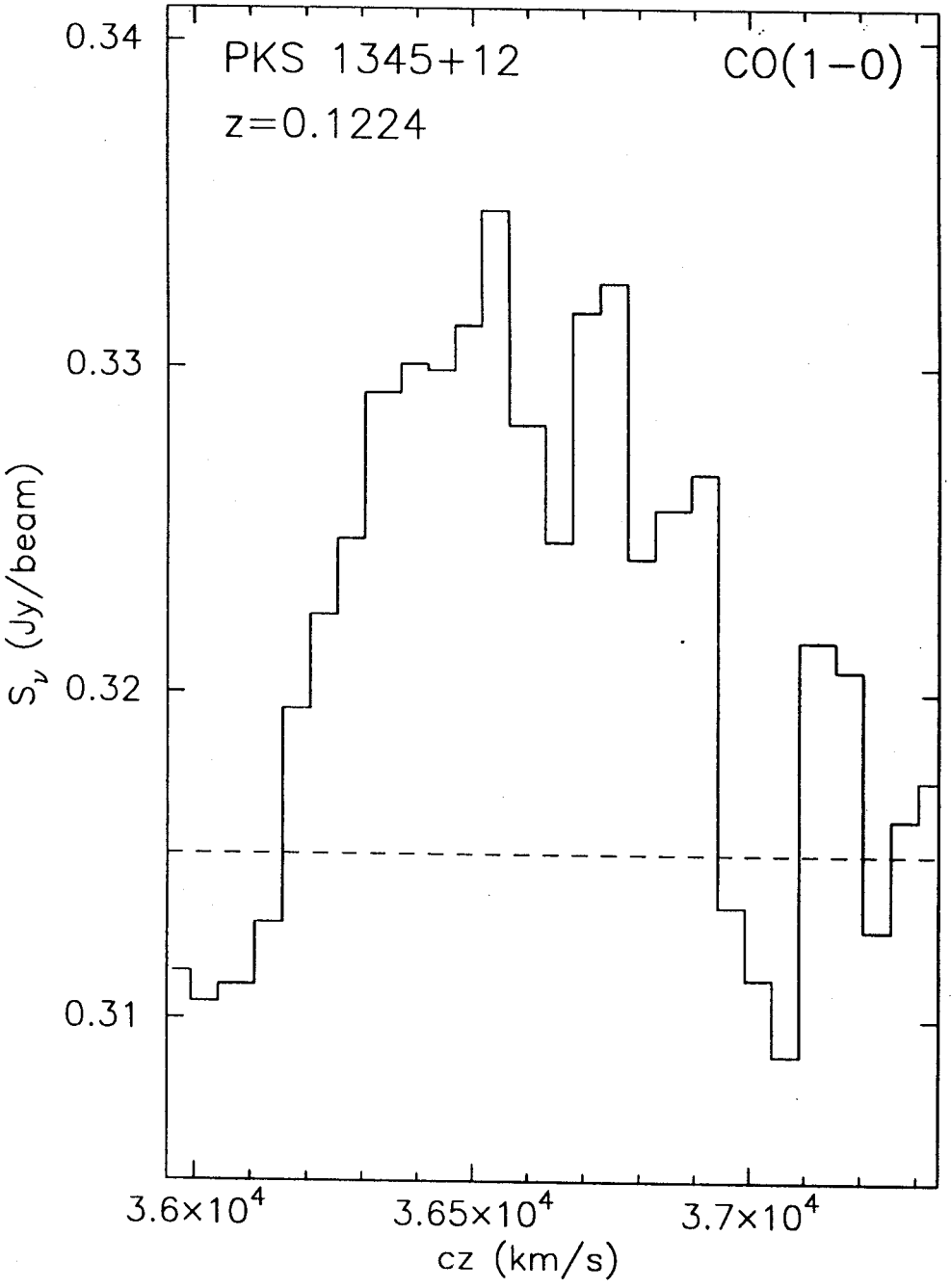
PKS 1345+12
CO(1−0)
z=0.1224
0.34
0.33
0.32
0.31
S_ν (Jy/beam)
3.6×10^4
3.65×10^4
3.7×10^4
cz (km/s)

Fig. 2